

Hyperfine spectroscopy of the $1s_5 - 2p_9$ transition of ^{39}Ar

J. Welte, I. Steinke, M. Henrich, F. Ritterbusch, M. K. Oberthaler, W. Aeschbach-Hertig, W. H. Schwarz, and M. Trieloff

Citation: *Review of Scientific Instruments* **80**, 113109 (2009); doi: 10.1063/1.3257691

View online: <https://doi.org/10.1063/1.3257691>

View Table of Contents: <http://aip.scitation.org/toc/rsi/80/11>

Published by the *American Institute of Physics*

Articles you may be interested in

[An efficient magneto-optical trap of metastable krypton atoms](#)

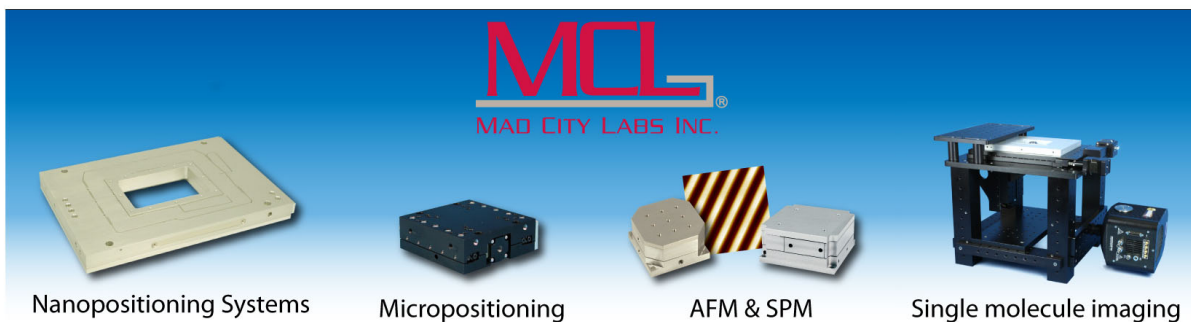
Review of Scientific Instruments **81**, 123106 (2010); 10.1063/1.3520133

[An atom trap system for practical \$^{81}\text{Kr}\$ dating](#)

Review of Scientific Instruments **75**, 3224 (2004); 10.1063/1.1790562

[Optical heterodyne saturation spectroscopy](#)

Applied Physics Letters **39**, 680 (1981); 10.1063/1.92867



Hyperfine spectroscopy of the $1s_5-2p_9$ transition of ^{39}Ar

J. Welte,^{1,a)} I. Steinke,¹ M. Henrich,¹ F. Ritterbusch,¹ M. K. Oberthaler,¹
W. Aeschbach-Hertig,² W. H. Schwarz,³ and M. Trieloff³

¹Kirchhoff-Institut für Physik, Universität Heidelberg, 69120 Heidelberg, Germany

²Institut für Umweltphysik, Universität Heidelberg, 69120 Heidelberg, Germany

³Institut für Geowissenschaften, Universität Heidelberg, 69120 Heidelberg, Germany

(Received 7 August 2009; accepted 11 October 2009; published online 19 November 2009)

We report on the first experimental determination of the hyperfine structure of the $1s_5-2p_9$ transition in ^{39}Ar . We give a detailed description of the sample preparation, spectroscopy cell cleaning, and spectroscopic setup. The resulting set of parameters consists of the hyperfine constants of the levels involved and the isotopic shift between ^{39}Ar and ^{40}Ar . With the achieved precision all laser frequencies necessary for the implementation of atom trap trace analysis for ^{39}Ar , i.e., laser cooling and repumping frequencies, are now known. © 2009 American Institute of Physics.

[doi:10.1063/1.3257691]

I. INTRODUCTION

The radioactive isotope ^{39}Ar ($T_{1/2}=269$ a,¹) has enormous potential in environmental physics bridging the dating gap between 50 and 1500 years. This timescale is of interest for many aspects connected to water cycles such as ocean circulation, continental glaciers, and water management.² Ultra-sensitive methods for ^{39}Ar detection already exist³⁻⁵ but incorporate very involved experimental effort. The application as a standard dating tracer may become feasible by realizing atom trap trace analysis (ATTA) for ^{39}Ar . ATTA has been demonstrated for rare isotopes of Kr (Ref. 6) and Ca (Ref. 7) and relies on the precise knowledge of the optical transition frequencies of the corresponding isotope. We report on the accurate determination of the hyperfine structure (hfs) of the relevant laser cooling transition. We access the hfs spectrum by means of modulation transfer laser spectroscopy in a glass spectroscopy cell with an external cavity diode laser at 811.7 nm. It contains an isotopically enriched sample of approximately 3 nLSTP (nanolitres at standard temperature and pressure) ^{40}Ar and 2.5 nLSTP ^{39}Ar resulting in a total pressure of $\sim 2.5 \times 10^{-4}$ mbar.

II. EXPERIMENTAL SETUP

A. Sample preparation

The gas sample is extracted from 410 mg potassium-rich mineral (HD-B1 biotite with $\sim 8\%$ K,⁸) which has been irradiated in the neutron reactor at the GKSS Research Centre Geesthacht (fast neutron flux: 10^{12} s⁻¹ cm⁻²) for 20 days leading to the production of ^{39}Ar by $^{39}\text{K}(n,p)^{39}\text{Ar}$. The neutron irradiation also induces production of short lived radioisotopes which have sufficiently decayed after an additional period of ~ 25 days. The irradiated sample is vacuum melted, the gas purified, and subsequently transferred via a zeolite-filled cold finger at $1N_2$ temperature to the specially

designed spectroscopy cell. For further details of sample preparation, neutron irradiation, argon extraction, and cleaning, see Ref. 9. The mineral also contains ^{40}Ar from *in situ* ^{40}K decay ($T_{1/2} \sim 1.3$ Ga) leading to $^{39}\text{Ar}/^{40}\text{Ar} \sim 0.8$ as determined via mass spectrometry from a simultaneously irradiated HD-B1 sample.

B. Spectroscopy cell and cleaning procedure

A quartz glass cell attached to a metal glass adapter is used for spectroscopy. The cell is cleaned by employing a similar scheme as reported in Ref. 10. After rinsing the cell with sodium hydroxide solution and de-ionized water it is subjected to an ultrasonic bath of de-ionized water at 35 °C for 5–10 min and finally flushed with methanol and de-ionized water. This procedure is repeated several times. Subsequently the cell is attached to the vacuum system and baked out during evacuation (120 °C for 12 h). In the next step an argon gas discharge is used to clean the cell more thoroughly before filling it with the actual sample. This is done with commercially available argon of atmospheric isotopic composition. The rf discharge used to populate the metastable levels operates at a pressure of 10^{-2} mbar and causes implantation of argon atoms into the cell walls.¹¹ Consequently this argon is desorbed from the cell walls when the discharge is operated at substantially lower pressures ($\sim 10^{-4}$ mbar). The degassing problem is overcome by running a high power gas discharge (up to 80 W) for about half an hour followed by controlled evacuation with a turbo molecular pump down to pressures of 10^{-6} mbar or less. Laser spectroscopy of the $1s_5-2p_9$ transition in ^{40}Ar is used to deduce the pressure during outgassing. This procedure is repeated until the pressure increase by degassing is negligible. During the evacuations the gas from the cell was analyzed with a commercially available residual gas analyzer allowing to obtain quantitative information on its composition.

The rf plasma discharge is powered by a multivibrator circuit with vacuum tubes that operates at high peak voltages

^{a)}Electronic mail: hfsar39@matterwave.de.

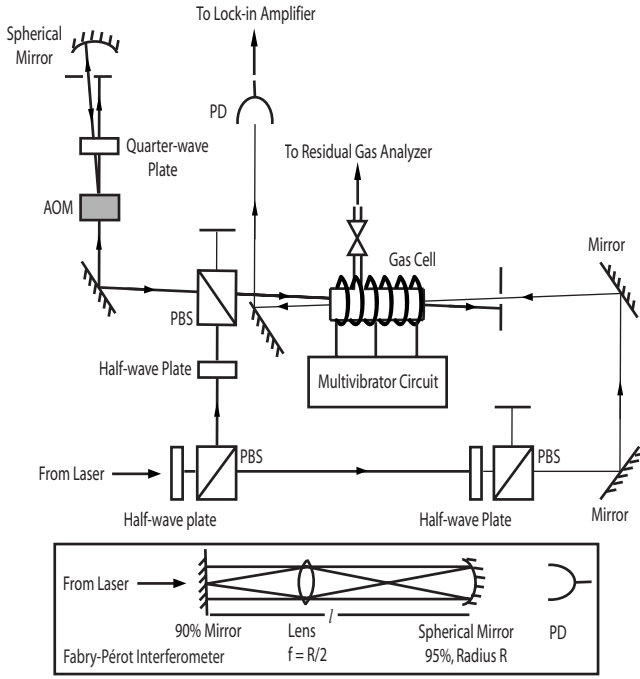


FIG. 1. The experiment is set up as Doppler-free saturation spectroscopy. The pump beam ($I=3 \cdot I_{\text{sat}}$) enters the cell from the left side after being frequency-modulated at 22 kHz with an amplitude of 10 MHz. The probe beam ($I=0.7 \cdot I_{\text{sat}}$) counterpropagates and is detected on a fast photodiode. The FPI has half the free spectral range of a confocal FPI due to the lens/mirror combination.

(up to 600 V,¹²). This high voltage allows for plasma ignition even at low densities since the acceleration forces on the charged particles are sufficiently strong.

C. Spectroscopy

We use modulation transfer Doppler-free saturation spectroscopy¹³ as depicted in Fig. 1. The pump beam is frequency modulated by a double pass acousto-optic modulator (AOM). The photodiode signal of the transmitted spectroscopy beam is demodulated using a lock-in amplifier and leads to a signal (derivative of the absorption profile) only at frequencies where both beams are resonant with the same velocity class of atoms. Since the laser linewidth is ~ 0.5 MHz and the gas pressure is low ($< 10^{-3}$ mbar) the predominant line broadening mechanisms are power broadening and modulation broadening. These effects result in a measured linewidth of 30 MHz whereas the natural linewidth of the transition is 5.85 MHz.¹⁴

The signal-to-noise ratio of the data is improved by averaging over many laser frequency scans. The spectroscopy signal in Fig. 2 thus corresponds to about 3200 single scans with 250 ms for each scan. The transmission signal of a Fabry-Pérot interferometer (FPI) is plotted and corresponds to a free spectral range $c/(8 \cdot l) = 83.3$ MHz due to the chosen design (lower part in Fig. 1). As the scan of the laser frequency deviates slightly from being linear the FPI peaks precisely determine a frequency scale. The ^{40}Ar peak is used as reference for averaging the single scans and thus allows for compensation of laser drifts.

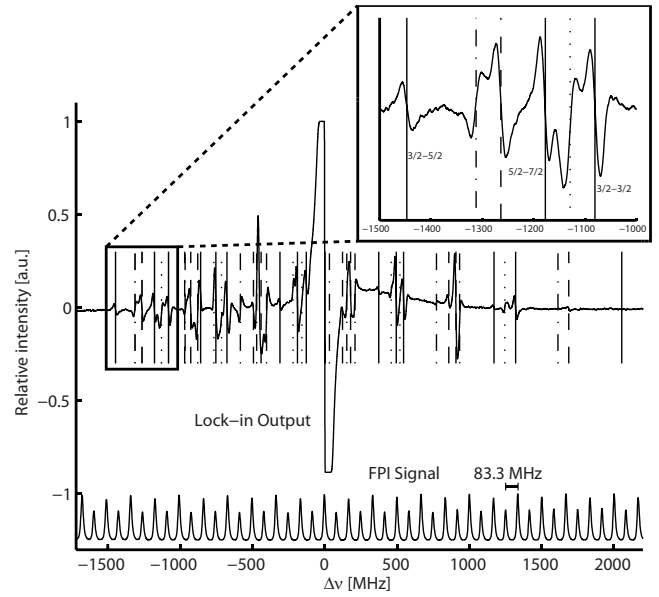


FIG. 2. The spectroscopy signal averaged over 3200 single scans. The vertical lines indicate the deduced resonances where the solid lines represent transitions between 2 hfs states; dashed: crossovers with adjacent excited levels; dash-dotted, dotted: other crossovers as indicated in Fig. 3.

III. DATA ANALYSIS AND RESULTS

The data are fitted with hyperfine splittings according to the hyperfine formula¹⁵ as follows:

$$\Delta E = \frac{A}{2}C + \frac{B}{4} \frac{\frac{3}{2}C(C+1) - 2I(I+1)J(J+1)}{I(2I-1)J(2J-1)}, \quad (1)$$

where J is the total angular momentum quantum number and I the nuclear spin. The magnetic dipole and electric quadrupole moments are expressed in the hyperfine constants A and B , respectively. The Casimir constant is defined as $C = F(F+1) - I(I+1) - J(J+1)$ where F is the coupling of J and I . With $I(^{39}\text{Ar}) = +7/2$, $J(1s_5) = 2$, and $J(2p_9) = 3$, the metastable state splits up into five levels from $F_s = 3/2$ to $11/2$ and the excited state splits up into seven levels from $F_p = 1/2$ to $13/2$.

This gives a set of 15 transitions according to selection rules. There are furthermore 10 crossover resonances between lines with the same hfs ground state. These 10 are not easily distinguishable from the other 15 lines as they have the same sign of slope. So the set of lines obtained from the spectrum was checked according to whether lines are right in-between two other lines. There are additional 20 lines which are also crossovers as illustrated in Fig. 3 but due to optical pumping rates they reveal an enhanced absorption leading to a derivative signal of opposite sign and thus are easily distinguished from the other resonances.

The hfs constants A_s , B_s , A_p , B_p and the—mainly mass-induced— isotopic shift $\Delta\nu$ are deduced by fitting the corresponding line positions. The isotopic shift was also estimated from the ratio of the shifts in other isotopes between the $1s_5-2p_9$ (Ref. 16) and the $1s_5-2p_6$ transition (Ref. 17) with help of the following empirical relation:

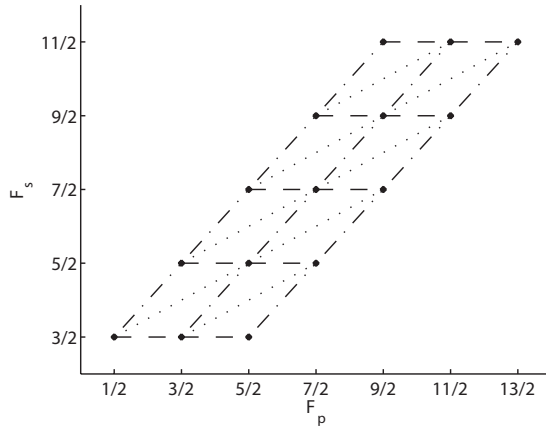


FIG. 3. This scheme describes the different types of observed and calculated transitions. Dots indicate transitions between two hfs levels, the lines of different style indicate different types of crossover resonance between two transitions as used in Fig. 2. Other resonances are also possible but are suppressed due to insufficient Doppler profile overlap.

$$\Delta\nu_{40}^{39}(1s_5 - 2p_9) = \frac{\Delta\nu_{40}^{\text{iso}}(1s_5 - 2p_9)}{\Delta\nu_{40}^{\text{iso}}(1s_5 - 2p_6)} \Delta\nu_{40}^{39}(1s_5 - 2p_6), \quad (2)$$

where $\Delta\nu_{40}^{\text{iso}}(1s_5 - 2p_{6/9})$ denotes the isotopic shift in the transition $1s_5 - 2p_{6/9}$ in the isotope $^{\text{iso}}\text{Ar}$ relative to the frequency of the same transition in ^{40}Ar . The corresponding data are given in Table I.

The hfs constants for the metastable state were estimated by Ref. 16 from measured data and for the excited state we made an empirical estimation with the help of data for other noble gas isotopes.^{18–31} Those estimated values are listed in Table II as well as the results from the fit. The lines calculated from the fitted parameters are plotted into Fig. 2. All observed features can be reproduced with the right slope (see Fig. 3).

IV. CONCLUSION

We have shown how to prepare and operate a low pressure gas discharge cell for noble gas isotopes with very limited availability. We solve the problem of igniting the discharge at low pressures as it is mentioned in Ref. 32 without adding carrier gases leading to undesirable contamination of the sample. In this context we developed a technique to reduce contamination and admixing from the cell walls due to

TABLE I. Isotopic shifts for different argon isotopes and two transitions. Equation (2) yields the shift in ^{39}Ar relative to ^{40}Ar and holds as the value for calculation from ^{36}Ar and ^{38}Ar is the same within the errors. The measured value agrees with the calculated value within errors.

Isotope	Transition	$\Delta\nu$ (MHz)	Ref.
36–40	$1s_5 - 2p_6$	$-494.9 \pm .6$	16
38–40	$1s_5 - 2p_6$	$-229.5 \pm .4$	
39–40	$1s_5 - 2p_6$	-107.1 ± 7.0	
36–40	$1s_5 - 2p_9$	$-450.1 \pm .9$	17
38–40	$1s_5 - 2p_9$	-208.1 ± 1.5	
39–40	$1s_5 - 2p_9$	-97.4 ± 6.4	Equation (2) for ^{36}Ar
39–40	$1s_5 - 2p_9$	-97.1 ± 6.4	Equation (2) for ^{38}Ar
39–40	$1s_5 - 2p_9$	$-95.0 \pm .4$	measured

TABLE II. Data for the hyperfine constants of the $1s_5$ and $2p_9$ levels of ^{39}Ar as estimated and for the first time directly measured experimentally. The larger errors on the B's result from Eq. (1) being much less sensitive to B than to A.

	Estimation	This work
A_s (MHz)	-286.1 ± 1.4^a	$-287.15 \pm .14$
B_s (MHz)	118 ± 20^a	119.3 ± 1.5
A_p (MHz)	-133 ± 14^b	$-135.16 \pm .12$
B_p (MHz)	115 ± 3^b	113.6 ± 1.9

^aSee Ref. 16: analysis using data from ^{37}Ar .

^bEstimated from the hfs constants of other noble gas isotopes.

desorption. With the first direct measurement of the hfs of ^{39}Ar all necessary laser frequencies for the implementation of ^{39}Ar -ATTA are now known.

ACKNOWLEDGMENTS

J. Tomkovič was of great help while dealing with data acquisition. H. Westphal provided us with great support during the design of the high power rf generator.

This work was partly funded by Landesstiftung Baden-Württemberg and Deutsche Forschungsgemeinschaft (DFG). J.W. gratefully acknowledges support through the graduate scholarship program of Baden-Württemberg.

- ¹R. W. Stoenner, O. A. Schaeffer, and S. Katcoff, *Science* **148**, 1325 (1965).
- ²H. Loosli, *Earth Planet. Sci. Lett.* **63**, 51 (1983).
- ³H. Loosli, M. Möll, H. Oeschger, and U. Schotterer, *Nucl. Instrum. Methods Phys. Res. B* **17**, 402 (1986).
- ⁴P. Collon, W. Kutschera, and Z.-T. Lu, *Annu. Rev. Nucl. Part. Sci.* **54**, 39 (2004).
- ⁵P. Collon, M. Bichler, J. Caggiano, L. D. Cecil, Y. E. Masri, R. Golser, C. L. Jiang, A. Heinz, D. Henderson, W. Kutschera, B. E. Lehmann, P. Leleux, H. H. Loosli, R. C. Pardo, M. Paul, K. E. Rehm, P. Schlosser, R. H. Scott, W. M. Smethie, Jr., and R. Vondrasek, *Nucl. Instrum. Methods Phys. Res. B* **223**, 428 (2004).
- ⁶C. Y. Chen, Y. M. Li, K. Bailey, T. P. O'Connor, L. Young, and Z.-T. Lu, *Science* **286**, 1139 (1999).
- ⁷I. D. Moore, K. Bailey, J. Greene, Z.-T. Lu, P. Mueller, T. P. O'Connor, C. Geppert, K. Wendt, and L. Young, *Phys. Rev. Lett.* **92**, 153002 (2004).
- ⁸J. C. Hess and H. J. Lippolt, *Compilation of K-Ar measurements of HD-BI standard biotite*, in Phanerozoic Time Scale, Bulletin of Liaison and Information of the I.U.G.S. Subcommittee on Geochronology, edited by G. S. Odin (1994), Vol. 12, pp. 19–23.
- ⁹W. H. Schwarz and M. Trieloff, *Chem. Geol.* **242**, 218 (2007).
- ¹⁰C. I. Sukenik and H. C. Busch, *Rev. Sci. Instrum.* **73**, 493 (2002).
- ¹¹X. Du, K. Bailey, Z.-T. Lu, P. Mueller, T. P. O'Connor, and L. Young, *Rev. Sci. Instrum.* **75**, 3224 (2004).
- ¹²S. Laue, M. Schüler, and H. Westphal, personal communication (2006).
- ¹³G. Camy, D. Pinaud, N. Courtier, and H. C. Chuan, *Rev. Phys. Appl.* **17**, 357 (1982).
- ¹⁴H. J. Metcalf and P. v. Straten, *Laser Cooling and Trapping* (Springer, New York, Berlin, Heidelberg, 1999).
- ¹⁵H. Kopfermann, *Kernmomente* (Akadem. Verl.-Ges, Frankfurt am Main, 1956).
- ¹⁶ISOLDE, A. Klein, B. Brown, U. Georg, M. Keim, E. Lievens, R. Neugart, M. Neuroth, R. Silverans, and L. Vermeeren, *Nucl. Phys. A* **607**, 1 (1996).
- ¹⁷G. D'Amico, G. Pesce, and A. Sasso, *J. Opt. Soc. Am. B* **16**, 1033 (1999).
- ¹⁸W. Traub, F. L. Roesler, M. M. Robertson, and V. W. Cohen, *J. Opt. Soc. Am.* **57**, 1452 (1967).
- ¹⁹X. Husson, J.-P. Grandin, and H. Kucal, *J. Phys. B* **12**, 3883 (1979).
- ²⁰B. D. Cannon and G. R. Janik, *Phys. Rev. A* **42**, 397 (1990).
- ²¹T. Trickle, M. J. J. Vrakking, E. Cromwell, Y. T. Lee, and A. H. Kung, *Phys. Rev. A* **39**, 2948 (1989).
- ²²J. R. Brandenberger, *Phys. Rev. A* **39**, 64 (1989).

- ²³G. D'Amico, G. Pesce, and A. Sasso, *Phys. Rev. A* **60**, 4409 (1999).
- ²⁴D. A. Jackson and M. C. Coulombe, *Proc. R. Soc. London, Ser. A* **335**, 127 (1973).
- ²⁵H. Gerhardt, F. Jeschonnek, W. Makat, E. Matthias, H. Rinneberg, F. Schneider, A. Timmermann, R. Wenz, and P. J. West, *Hyperfine Interact.* **9**, 175 (1981).
- ²⁶X. Husson and J. P. Grandin, *J. Phys. B* **11**, 1393 (1978).
- ²⁷R.-J. Champeau and J.-C. Keller, *J. Phys. B* **6**, L76 (1973).
- ²⁸T. W. Ducas, M. S. Feld, J. L. W. Ryan, N. Skribanowitz, and A. Javan, *Phys. Rev. A* **5**, 1036 (1972).
- ²⁹L. Julien, M. Pinard, and F. Laloë, *J. Phys. (Paris), Lett.* **41**, 479 (1980).
- ³⁰G. M. Grosof, P. Buck, W. Lichten, and I. I. Rabi, *Phys. Rev. Lett.* **1**, 214 (1958).
- ³¹S. Liberman, *Physica (Amsterdam)* **69**, 598 (1973).
- ³²K. Rudinger, Z.-T. Lu, and P. Mueller, *Rev. Sci. Instrum.* **80**, 036105 (2009).